



PERGAMON

Solid State Communications 113 (2000) 239–243

solid
state
communications

www.elsevier.com/locate/ssc

In-donor complexes in Si and Ge: structure and electric field gradients

A. Settels^{a,*}, K. Schroeder^a, T. Korhonen^b, N. Papanikolaou^a, M. Aretz^a,
R. Zeller^a, P.H. Dederichs^a

^a*Institut für Festkörperforschung, Forschungszentrum Jülich, D-52425 Jülich, Germany*

^b*Laboratory of Physics, Helsinki University of Technology, P.O. Box 1100, FIN-02015 Helsinki, Finland*

Received 13 September 1999; accepted 21 October 1999 by H. Eschrig

Abstract

The electronic and geometrical structure of neutral InD (D = P, As, Sb) acceptor–donor pairs in silicon and germanium is studied using two complementary ab-initio methods, i.e. the all-electron Korringa–Kohn–Rostoker (KKR) Green’s function method and the pseudopotential ab-initio molecular dynamics method. Furthermore the electric field gradients are predicted at the In sites, which can be measured by PAC experiments using the ¹¹⁷Cd/¹¹⁷In probe. The results for the InD pairs are compared with the geometrical structures and in particular with the electric field gradients of the isoelectronic [CdD][−] complexes in silicon and germanium. The lattice relaxations calculated by both theoretical methods for the InD complexes agree quite well and are similar to the relaxations for the [CdD][−] complexes, which have been studied extensively in PAC experiments using the ¹¹¹In/¹¹¹Cd probe. In contrast to this the calculated In electric field gradients are, however, considerably larger than the Cd ones. © 1999 Elsevier Science Ltd. All rights reserved.

Keywords: A. Semiconductors; C. Impurities in semiconductors; C. Point defects; E. Nuclear resonances

1. Introduction

If semiconductors are, intentionally or unintentionally, doped with both acceptor and donor atoms, the coulombic attraction leads to the formation of stable acceptor–donor complexes. Unfortunately very little experimental information exists about these complexes, since they are normally not electrically or magnetically active. One exception is perturbed $\gamma\gamma$ angular correlation (PAC) experiments, using the ¹¹¹In/¹¹¹Cd probe atom [1–5]. In these experiments the ¹¹¹In mother atom forms with the donor atom D = P, As or Sb a neutral pair complex [InD]⁰ on the nearest neighbor sites. After the decay ¹¹¹In → ¹¹¹Cd the electric field gradient (EFG) at the Cd site is measured, which then refers to the electronic structure of the CdD-complex, so that no direct information is obtained about the InD complex. In a recent paper [6] we have presented a detailed ab-initio study of these CdD-complexes in Si and Ge. The

calculated electric field gradients depend very sensitively on the lattice relaxations of the defect complex and good agreement with experiments is obtained if the complicated equilibrium structure is determined accurately. In the same paper we have also discussed the existence of two different charge states, [CdD]⁰ and [CdD][−], and of larger complexes ([CdD₂]⁰).

In this communication we would like to study the corresponding InD-complexes in Si and Ge. On the one hand it is interesting to study the differences and similarities between these mother complexes and the CdD daughter complexes, the electric field gradient of which are measured in the PAC experiments. On the other hand we have been informed that it is also possible to directly measure the electric field gradients of the InD-complexes, if one uses the ¹¹⁷Cd/¹¹⁷In probe atom [7], where the role of the mother and daughter nucleus is exchanged. For these reasons we present here predictions for the EFGs of these In complexes, hoping that such experiments will be performed in the future. Finally we want to point out that the InD pairs present also an interesting test case for the theory, since

*Corresponding author.

the low lying 4d-semicore states of the In atoms allow the application of standard pseudopotential techniques. Therefore, we present here a critical comparison of the complicated defect structures calculated by two complementary methods: (1) the all-electron KKR Green's function method which takes the full anisotropy of the potential into account and (2) the pseudopotential ab-initio molecular dynamics method, allowing a completely different evaluation of the lattice relaxations. As we will show below, both methods give very similar results. However, unfortunately, only the first method allows a calculation of the EFGs, being determined by the behavior of the valence and semicore p-states in the inner core region.

2. Theoretical methods

For both ab-initio methods the theoretical approach is based on the density-functional theory in the local density approximation (LDA) as parametrized by Vosko et al. [8].

Within the KKR Green's function method [9–11] a crystalline solid is divided into non-overlapping and space-filling cells around each atomic site. In this multiple scattering approach the perturbed region around a defect complex is exactly embedded in the unperturbed crystal. The fundamental density-functional quantity, i.e. the charge density, can be calculated from the imaginary part of the Green's function by a contour integral in the complex energy plane. In the KKR calculations the LDA lattice constants (for Si: 5.40 Å and for Ge: 5.57 Å) as calculated in [12] are used and the diamond lattice structure is described using four basis positions along the [111] direction, two for the Si or Ge atoms and two empty sites. For the substitutional InD pairs along the [111] direction a cluster of 76 perturbed potentials (38 atoms) with C_{3v} symmetry is embedded in the unperturbed ideal host crystal. In the KKR technique the forces are calculated via a so-called "ionic" Hellmann–Feynman (HF) [13] theorem. To treat lattice relaxations firstly the host quantities, like Green's function and potentials, have to be transformed relative to the new positions as it is described in Ref. [13]. Secondly the l-expansion of the shape functions, describing the proper shapes of the Wigner–Seitz cells, has to be adjusted to the new positions. For large lattice relaxations we perform a Voronoi construction for the cellular division around the shifted positions, to ensure that each atom sits at the center of a cell with a relative high local symmetry, which facilitates the l convergence. The angular momentum expansion is cut-off at $l_{max} = 4$, which has proven to be more than enough for sp bonded materials [14].

The pseudopotential calculations were performed using ESTCOMP [15], a self developed ab initio molecular dynamics program in the spirit of Car and Parinello [16], based on the local density approximation (LDA) [8,17] to the density functional theory (DFT) using norm-conserving pseudo-potentials [18,19] of the Kleinman–Bylander form

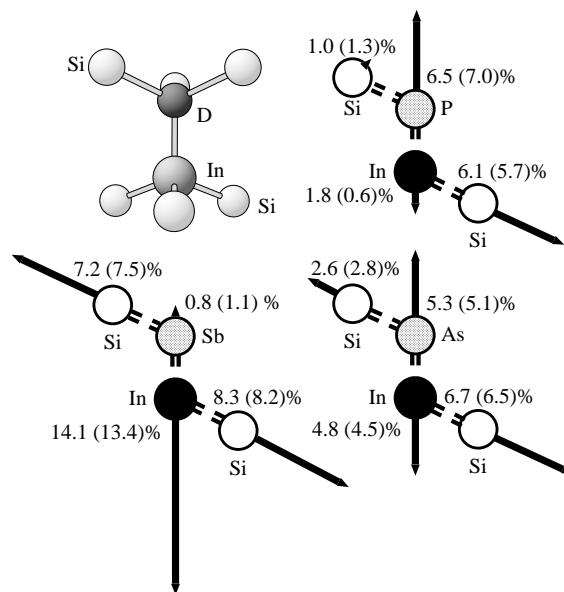


Fig. 1. Lattice relaxations for the defect atoms and the nn atoms of $[\text{InD}]^0$ (D = P, As, Sb) defect pairs in Si, calculated via KKR and pseudopotential techniques. Shown are the three-dimensional arrangement of the InD complex (top, left-hand) and the (110) planes containing the InD-pairs and the two representative Si neighbors. Relaxations are given in percentage of the NN-distance. The first number refers to the relaxation obtained by the KKR Green's function method, the second number (in brackets) to the pseudopotential results.

[20], a plane-wave basis set for the wave functions and iterative diagonalization schemes [21] for the eigenvalue problem. The convergence of the charge density to self-consistency is accelerated by quasi-Newton methods [22]. Forces are calculated and fed into a quasi-Newton-scheme to determine the minimum energy configurations.

The Si(Ge) crystal is simulated by a super cell containing 64 atoms, centered around the InD pair. We used a \mathbf{k} -point set equivalent to $6 \times 6 \times 6$ \mathbf{k} -points in the BZ of the bulk and a plane-wave cut-off $E_{max} = 11.56Ry$. For regular runs the In-donor-pair and six nearest neighbors (NN) were allowed to relax. For several InD pairs we also performed calculations with a (111)-oriented cell centered around the InD-pair-axis (containing 108 atoms) and allowed the nNN-atoms (in total 50 atoms) to relax. The resulting relaxations for the pair and NN-atoms were equal to the results of the smaller cell within 0.01 Å, i.e. 0.2% of the cubic lattice constant.

3. Lattice relaxations of the InD complexes

The calculated equilibrium structures for the InP, InAs and InSb complexes in Si are shown in Fig. 1. The upper left figure illustrates the geometric environment of the InD pairs, whereas the other pictures show the relaxations of the

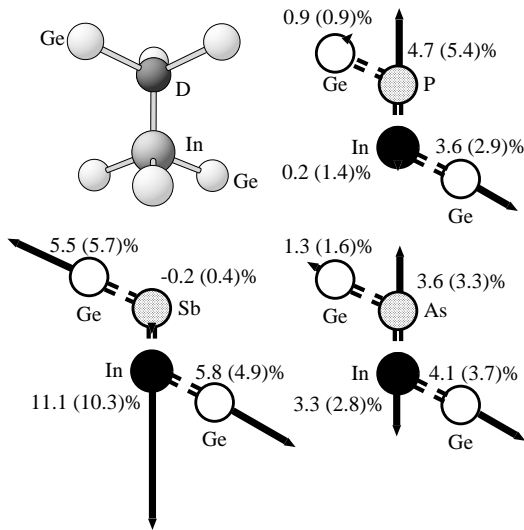


Fig. 2. Lattice relaxations for the defect atoms and the NN atoms of $[InD]^0$ ($D = P, As, Sb$) defect pairs in Ge, calculated via KKR and pseudopotential techniques. See Fig. 1 for a more detailed description.

pair atoms and the two representative Si neighbors in the (110) plane. The arrows indicate the size and direction of the relaxations, whereas the numbers give the absolute value of the relaxation in percent of the Si nearest neighbor distance, with the first number referring to the KKR results and the second (bracketted) number to the ab-initio MD values. As one can see, both values, obtained by completely different electronic structure methods, are always very similar. Typically the KKR relaxations of the In atoms are slightly larger than the one obtained from the pseudopotential method. However, in total these differences are small showing the reliability and accuracy of both methods. The geometric arrangement of the pairs is dictated by the sizes of the In and donor atoms. For instance, the In atom pushes

the small donor atom P by 6.5% away from the ideal position, while on the other hand the heavier Sb atom is shifted only slightly, but pushes the In atoms away by 14%. In contrast to this, the InAs complex is rather symmetrical. The relaxations, shown in Fig. 1 for the InD complexes, are similar to the relaxations obtained in [6] for the negatively charged $[CdD]^-$ complexes in Si. The main difference arises from the somewhat smaller size of the Cd atom, resulting in somewhat smaller relaxations. For instance in the $[CdSb]^-$ complex the Cd–Sb distance is 13.5% larger than the NN distance, compared to 14.9% for the In–Sb distance in the $[InSb]^0$ complex. However for the neutral $[CdSb]^0$ complex the relaxations are considerably different and we will come back to these differences in the discussion of the EFGs.

Fig. 2 shows the relaxation pattern for the InD complexes in Ge. The basic features are similar to the ones shown in Fig. 1 for the Si host, except that all relaxations are reduced, which is a consequence of the 4% larger lattice constant of Ge. Also in the Ge case the relaxations of the InD complexes are similar to, but somewhat larger than, the relaxations for the corresponding $[CdSb]^-$ pairs in Ge, and as above the results obtained by the KKR and the pseudopotential method agree quite well.

Another feature, which can be seen from Figs. 1 and 2, is that the pair distances In–D want to restore the corresponding nearest neighbor distances of the bulk semiconductors InP, InAs and InSb. For instance in Si the pair distances are for InP 8.3(7.6)%, for InAs 10.1(9.6)% and for InSb 14.9(14.5)% larger than the NN distance of Si, whereas the corresponding numbers for the bulk semiconductors are: InP 8.5%, InAs 11% and InSb 19.5%.

4. Electric field gradients of the InD complexes

Table 1 shows the calculated EFGs for the $[InD]^0$ complexes in Si and Ge at the In sites in units of

Table 1

The largest eigenvalue V_{zz} of the electric field gradient tensor in 10^{21} [V/m²] at the In site for $[InD]^0$ pairs in silicon and germanium. $EFG_{relaxed}^{KKR}$ denotes the KKR calculation and $EFG_{relaxed}^{PSEUDO}$ an all-electron KKR calculation using the positions obtained by a pseudopotential technique. In all calculations the asymmetry parameter $\eta = 0$ vanishes for symmetry reasons. The table also includes the EFGs for the $[CdD]^-$ complexes in Si and Ge as calculated in [6] and as obtained experimentally [1,4]

	EFG_{ideal}	$EFG_{relaxed}^{KKR}$	$EFG_{relaxed}^{PSEUDO}$		$EFG_{relaxed}^{KKR}$	EFG_{exp}
Si-Host						
$[InP]^0$	-14.4	-18.5	-17.2	$[CdP]^-$	-9.5	-8.9
$[InAs]^0$	-12.8	-19.8	-19.3	$[CdAs]^-$	-12.4	-11.4
$[InSb]^0$	-3.9	-20.6	-20.3	$[CdSb]^-$	-14.6	-13.5
Ge-Host						
$[InP]^0$	-11.2	-13.9	-12.3	$[CdP]^-$	-6.2	-4.3
$[InAs]^0$	-10.1	-15.8	-15.1	$[CdAs]^-$	-9.1	-7.3
$[InSb]^0$	-2.1	-16.1	-15.9	$[CdSb]^-$	-11.7	-10.1

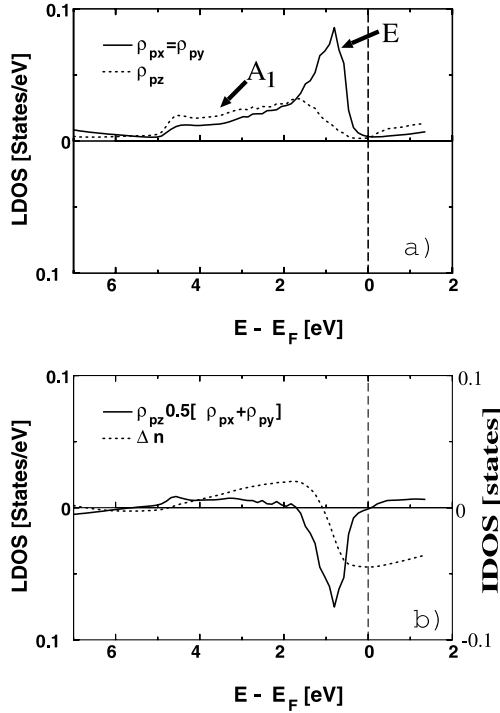


Fig. 3. (a) Projected local density of states $\rho_{pz}(E)$ (A_1 subspace) and $\rho_{px}(E) = \rho_{py}(E)$ (E -subspace) on the In site (the z -axis points to the donor atom). Note the difference in the DOS form and the population of the p_z and p_x, p_y orbitals. (b) Anisotropic contribution $\Delta\rho_p(E) = \rho_{pz}(E) - \frac{1}{2}[\rho_{px}(E) + \rho_{py}(E)]$ to local p DOS at the In site. The dashed curve Δn_p represents the integrated DOS (IDOS) ($\Delta n_p(E) = \int^E dE' \Delta\rho_p(E')$), the value $\Delta n_p(E_F)$ of which determines the EFG of the In atom.

10^{21} V/m^2 . The EFG values are given in Table 1 for the ideal positions (EFG_{ideal}), as well as for the equilibrium positions obtained using the KKR technique (EFG_{relaxed}^{KKR}) or the pseudopotential technique (EFG_{relaxed}^{PSEUDO}). For the latter the positions obtained by pseudopotential calculations were used to calculate the EFG via the all-electron KKR method. Furthermore the corresponding EFGs for [CdD]⁻ complexes in Si and Ge are listed in Table 1 as determined by the KKR method (EFG_{relaxed}^{KKR}) [6] and by experiments (EFG_{exp}) [1,4].

Without lattice relaxations we get a totally wrong trend for the EFG at the In site. Even a decrease for the EFG in the sequence InP, InAs, InSb is obtained. In the relaxed geometry this trend is changed to an increasing EFG with increasing donor size. The agreement between EFG_{relaxed}^{KKR} and EFG_{relaxed}^{PSEUDO} is good. The small difference arises from the uncertainty to determine the correct equilibrium positions (compare Figs. 1 and 2) for the relaxations of the pair atoms and the nearest neighbors by both methods. In all three cases the lattice relaxations in the KKR method are a bit larger than the pseudopotential calculation. Due to this, the electric field gradients are slightly higher for the positions obtained in the KKR calculation. Compared to the

[CdD]⁻ complexes in silicon and germanium the EFGs are considerably larger for the InD pairs, which will be explained below. Furthermore the differences in the EFGs for the different donor atoms P, As and Sb are considerably smaller for the In than for the Cd complexes.

Following Blaha et al. [23] the electric field gradient V_{zz} is in a good approximation proportional to the population anisotropy of the In p-valence charges:

$$V_{zz} \propto \Delta n_p = n_{pz} - \frac{1}{2}(n_{px} + n_{py}), \quad (1)$$

where the z -axis points in the [111] (pair) direction. For an understanding of the origin of the EFG the corresponding projections of the local p density of states along the [111] direction, $\rho_{pz}(E)$, and perpendicular to [111], $\rho_{px}(E)$ and $\rho_{py}(E)$, at the In site are shown in Fig. 3(a) for the InAs complex. The corresponding population anisotropy DOS $\Delta\rho_p(E)$ and the integrated p anisotropy DOS $\Delta n_p(E) = \int^E dE' \Delta\rho_p(E')$ is shown in Fig. 3(b). The origin of the electric field gradient results from a different population of the p_x, p_y and p_z orbitals, which can be understood by a simple hybridisation model [6]. For a substitutional In⁻ acceptor the EFG vanishes due to the isotropic p charge density. The pair formation leads to a symmetry induced splitting of the T_2 acceptor level (T_d notation for the symmetry of an isolated acceptor) into a A_1 and a E level (C_{3v} notation for the symmetry of the pair complex). For symmetry reasons only the A_1 (T_d and C_{3v}) level of the donor atom. As can be seen from Fig. 3(a) the p_z charge along [111] exhibits A_1 symmetry, whereas the perpendicular p_x and p_y charges belongs to the E subspace. Due to the hybridisation the A_1 bonding level is shifted into the valence bands and the antibonding A_1 level in the conduction bands, while the E level is practically not affected. Therefore, only the p_z charge at the In site is decreased and transferred via hybridisation into the A_1 charge at the donor site. This leads to an anisotropic p-charge distribution as it can be seen from Fig. 3(b). In general the origin for the EFG is the same for the [InD]⁰ pairs as for the [CdD]⁻ complexes. But there are, of course, some differences between the In and the Cd acceptor, which lead to different quantitative results. First the In p-states are lower in the energy, in particular there are no states in the bandgap. In both cases all E -states are occupied (i.e. by four electrons) so that the pairs are iso-electronic. Therefore, the [InD]⁰ pairs are neutral and the [CdD]⁻ complexes negatively charged. These states are, however, very extended. Due to the lower p-levels of the In atom, locally on the In sites the p occupancy is a bit larger, e.g. for [InAs]⁰ in Si $n_p^{Si} = 0.84$ compared to $n_p^{Si} = 0.64$ for [CdAs]⁻ in Si. But more important is, however, the stronger anisotropy of the p-charges of In as compared to Cd, e.g. for [InAs]⁰ in Si (see Fig. 3b) $\Delta n_p(E_F) \approx 0.044[\text{states}]$ compared to $\Delta n_p(E_F) \approx 0.029[\text{states}]$ for [CdAs]⁻ in Si.

Thus the stronger anisotropy of the p-charge density at the In sites increases the EFGs as compared to the isoelectronic Cd complexes. The reason for that is the stronger hybridisation of the In p_z level with the A_1 -level of the donor atoms, which leads to a stronger decrease of n_{pz} as compared to Cd pairs.

5. Conclusions

We performed ab-initio calculations of the electronic structure, lattice relaxations and electric field gradients of InD acceptor–donor complexes in Si and Ge. The complex pattern of lattice relaxations is somewhat larger for InD than for the corresponding $[\text{CdD}]^-$ complexes, studied earlier [6]. We obtain a very good agreement between lattice relaxations determined by the full potential KKR Green's function method and the pseudopotential ab-initio MD method. We predict EFGs for the InD complexes, which are considerably larger than the EFGs of the isoelectronic $[\text{CdD}]^-$ complexes, due to stronger hybridisation with the A_1 state of the donors. Our calculations for the InD and the CdD [6] complexes in Si and Ge give a consistent picture of the properties of acceptor–donor complexes in Si and Ge. In order to confirm these theoretical results measurements of the EFGs of the InD complexes would be very helpful.

Acknowledgements

We want to acknowledge discussions with D. Forkel-Wirth. This work was funded by the Federal Ministry for Science and Technology (BMBF, Contract No. 05606CJA3).

References

[1] Th. Wichert, M.L. Swanson, J. Appl. Phys. 66 (1989) 3026.

- [2] Th. Wichert, M. Grübel, G. Keller, N. Schulz, H. Skudlik, Appl. Phys. A48 (1989) 59.
- [3] Th. Wichert, in Semiconductors and Semimetals (Academic Press, Volume 51B Chapter 6, 1999).
- [4] D. Forkel, N. Achtziger, A. Baurichter, M. Deicher, S. Deubler, M. Puschmann, H. Wolf, W. Witthuhn, Nucl. Instr. Meth. in Phys. Res. B63 (1992) 217.
- [5] N. Achtziger, W. Witthuhn, Phys. Rev. B 47 (1993) 6990.
- [6] A. Settels, T. Korhonen, N. Papanikolaou, R. Zeller, P.H. Dederichs, Phys. Rev. Lett. (1999), in press.
- [7] D. Forkel-Wirth, private communication.
- [8] S.H. Vosko, L. Wilk, M. Nusair, Can. J. Phys. 58 (1980) 1200.
- [9] J. Korringa, Physica 13 (1947) 392.
- [10] W. Kohn, N. Rostoker, Phys. Rev. 94 (1954) 1111.
- [11] P.J. Braspenning, R. Zeller, A. Lodder, P.H. Dederichs, Phys. Rev. B 29 (1984) 703.
- [12] M. Asato, A. Settels, T. Hoshino, T. Asada, S. Blügel, R. Zeller, P.H. Dederichs, Phys. Rev. B 60 (1999) 5202.
- [13] N. Papanikolaou, R. Zeller, P.H. Dederichs, N. Stefanou, Phys. Rev. B 55 (1997) 4157.
- [14] A. Settels, Ph.D. thesis RWTH Aachen, 1999 (unpublished).
- [15] ESTCOMP: Electronic Structure Code for Materials Properties and Processes, Forschungszentrum Jülich, 1999. A parallelized version of this program is available (see R. Berger et al., Proceedings of the NIC-Workshop "Molecular Dynamics on parallel Computers", Jülich, 08.-10. Februar 1999, World Scientific 1999).
- [16] R. Car, M. Parrinello, Phys. Rev. Lett. 55 (1985) 2471.
- [17] L. Hedin, B.I. Lundqvist, J. Phys. C 4 (1971) 2064.
- [18] G.B. Bachelet, D.R. Hamann, M. Schlüter, Phys. Rev. B 26 (1982) 4199.
- [19] A.M. Rappe, K.M. Rabe, E. Kaxiras, J.D. Joannopoulos, Phys. Rev. B 41 (1990) 1227.
- [20] L. Kleinman, D.M. Bylander, Phys. Rev. Lett. 48 (1982) 1425.
- [21] N. Kosugi, J. Comput. Phys. 55 (1984) 426.
- [22] S. Blügel, PhD thesis, RWTH Aachen, 1988 (unpublished).
- [23] P. Blaha, K. Schwarz, P.H. Dederichs, Phys. Rev. B 37 (1988) 2792.